

Boron Complexes with Mesityl and Oxyquinoline Ligands: Syntheses, Structures, and Luminescence Properties

A. V. Rozhkov^a, E. V. Baranov^{a, b}, V. A. Il'ichev^{a, b}, A. O. Korshunov^{a, b}, and L. N. Bochkarev^{a, b, *}

^a G.A. Razuvayev Institute of Organometallic Chemistry, Russian Academy of Sciences,
ul. Tropinina 49, Nizhny Novgorod, 603600 Russia

^b Nizhny Novgorod State University, pr. Gagarina 23, Nizhny Novgorod, 603600 Russia

*e-mail: lnb@iomc.ras.ru

Received March 4, 2015

Abstract—New oxyquinoline boron complexes Mes_2BQ (**I**) and $\text{Mes}_2\text{BQ}^{\text{Me}}$ (**II**), where QH is 8-hydroxyquinoline and $\text{Q}^{\text{Me}}\text{H}$ is 2-methyl-8-hydroxyquinoline, (CIF files CCDC 1051351 (**I**) and 1051352 (**II**)) are synthesized and structurally characterized. Their photoluminescence (PL) and electroluminescence (EL) properties are studied. The compounds have an intense green PL. The EL characteristics of complexes **I** and **II** doped in poly-N-vinylcarbazole (PVK) differ substantially. Compound **I** generates green luminescence with a brightness of 356 cd/m^2 , whereas white EL with a brightness of 36 cd/m^2 is observed in the case of compound **II**.

DOI: 10.1134/S1070328415100061

INTRODUCTION

It is known that some boron complexes with chelating O,O- and N,O-ligands manifest efficient EL properties and can generate radiation in the blue, green, and red spectral ranges [1, 2]. As compared to the presently known most efficient electrolumino-phores based on the iridium and platinum compounds [3, 4], the organoboron emitters are favorable due to a significantly lower cost, a less labor-consuming synthesis, and the absence of toxic properties. Therefore, studies on the synthesis of new electroluminescent boron compounds are being continuously developed. The EL efficiency and color of organoboron emitters are determined, to a significant extent, by the nature of the ligands bound to the boron atom. It was shown in a series of works that the inclusion of oxyquinoline and aryl ligands into the boron complexes induced efficient EL properties in these complexes [5–7].

In this work, we report the syntheses, structures, and the PL and EL properties of the new boron complexes with mesityl and 8-oxyquinoline ligands.

EXPERIMENTAL

All procedures with easily oxidizable and hydrolyzable substances were carried out in *vacuo* or in argon according to the standard Schlenk procedure. The solvents used were thoroughly purified and degassed. Fluorodimesitylborane (Mes_2BF) was synthesized using a known procedure [8]. 8-Hydroxyquinoline (QH), 2-methyl-8-hydroxyquinoline ($\text{Q}^{\text{Me}}\text{H}$), aluminum *tris*(8-oxyquinolate) (Alq_3), poly-N-vinylcarbazole (PVK), and 4,7-diphenyl-1,10-phenanthroline

(BATH) (Aldrich) were used without additional purification.

^1H , ^{13}C , and ^{11}B NMR spectra were recorded on a Bruker Avance III–400 spectrometer (^1H NMR: 400 MHz, ^{13}C NMR: 100 MHz, ^{11}B NMR: 128 MHz). Chemical shifts were given in ppm relative to tetramethylsilane as an internal standard. IR spectra were measured on an FSM 1201 FTIR spectrometer. Samples of complexes **I** and **II** were prepared by pressing pellets (ratio substance : KBr = 1 : 200).

Electronic absorption spectra were recorded on a PerkinElmer Lambda 25 UV/VIS spectrometer. Photoluminescence spectra were obtained on a Perkin Elmer LS 55 fluorescence spectrometer. The relative quantum yield in a CH_2Cl_2 solution was determined at room temperature (excitation wavelength 360 nm). The values of quantum yields were calculated relative to Rhodamine 6G in alcohol ($\Phi = 0.95$) [9] using a known procedure [10].

Electroluminescence spectra, current density-voltage and luminance-voltage characteristics, and CIE chromaticity coordinates were obtained on model OLED devices without encapsulation using an automated computer-conjugated complex including a GW INSTEK PPE-3323 power source, a GW INSTEK GDM-8246 digital multimeter, and an Ocean Optics USB 2000 spectrofluorimeter.

Synthesis of Mes_2BQ (I**).** A suspension of NaH (0.018 g, 0.74 mmol) in THF (3 mL) was added to a solution of QH (0.11 g, 0.74 mmol) in THF (6 mL). The mixture was stirred at room temperature for 2 h. The obtained solution of the sodium salt was added by

portions to a solution of Mes_2BF (0.20 g, 0.74 mmol) in THF (5 mL), and the mixture was stirred at room temperature for 6 h. The solvent was removed by evaporation in vacuo, and the residue was extracted with toluene (3×5 mL). After the solvent was removed, the residue was recrystallized from CH_2Cl_2 . Complex **I** was obtained as light yellow crystals. The yield was 0.28 g (96%).

IR (KBr; ν , cm^{-1}): 3055, 1624, 1610, 1579, 1551, 1504, 1423, 1331, 1123, 1027, 878, 846, 816. ^1H NMR (CDCl_3 ; δ , ppm): 8.78 (dd, $J = 4.2$ and 1.5 Hz, 1 H), 8.17 (dd, $J = 8.3$ and 1.5 Hz, 1 H), 7.51–7.41 (m, 2 H), 7.34 (dd, $J = 8.3$ and 1.1 Hz, 1 H), 7.19 (dd, $J = 7.6$ and 1.1 Hz, 1 H), 6.77 (d, $J = 39.6$ Hz, 4 H), 2.32–2.22 (m, 18 H). ^{13}C NMR (CDCl_3 ; δ , ppm): 152.3, 147.8, 141.1, 138.9, 138.4, 136.1, 128.7, 127.8, 121.8, 117.9, 109.9, 22.4, 21.2. ^{11}B NMR (CDCl_3 ; δ , ppm): 15.98.

For $\text{C}_{27}\text{H}_{28}\text{BNO}$

| | | |
|-------------------|-----------|----------|
| anal. calcd. (%): | C, 82.45; | H, 7.18. |
| Found (%): | C, 82.44; | H, 7.16. |

Synthesis of $\text{Mes}_2\text{BQ}^{\text{Me}}$ (II) was carried out similarly to the procedure described above. Complex **II** was obtained as light yellow crystals. The yield was 0.26 g (88%).

IR (KBr; ν , cm^{-1}): 3272, 3024, 1608, 1573, 1508, 1429, 1328, 1258, 1218, 1196, 1161, 1094, 1029, 958, 869, 844, 832, 795. ^1H NMR (CDCl_3 ; δ , ppm): 8.04 (d, $J = 8.4$ Hz, 1 H), 7.42–7.35 (m, 1 H), 7.34–7.26 (m, 2 H), 7.14 (dd, $J = 7.5$ and 1.1 Hz, 1 H), 6.81 (d, $J = 7.3$ Hz, 4 H), 2.73 (s, 3 H), 2.26 (dd, $J = 11.0$ and 5.0 Hz, 18 H). ^{13}C NMR (CDCl_3 ; δ , ppm): 156.6, 141.6, 137.7, 136.6, 131.2, 128.4, 126.9, 126.7, 125.1, 122.7, 117.5, 115.2, 109.9, 29.7, 24.9, 21.2. ^{11}B NMR (CDCl_3 ; δ , ppm): 50.41.

For $\text{C}_{28}\text{H}_{30}\text{BNO}$

| | | |
|-------------------|-----------|----------|
| anal. calcd. (%): | C, 82.56; | H, 7.42. |
| Found (%): | C, 82.51; | H, 7.40. |

X-ray diffraction analysis. The crystallographic data for compounds **I** and **II** were obtained on Bruker AXS D8 Quest Photon (for **I**) and Oxford Xcalibur Eos (for **II**) automated diffractometers (MoK_α radiation, ω scan mode, $\lambda = 0.71073$ Å). Reflection intensities were processed using the SAINT [11] (**I**) and CrysAlisPro [12] (**II**) programs. The SADABS [13] (**I**) and SCALE3 ABSPACK [14] (**II**) programs were used to apply absorption corrections. The structures were solved by a direct method (SHELXTL) [15] and refined by full-matrix least squares in the anisotropic approximation for all non-hydrogen atoms. Hydrogen

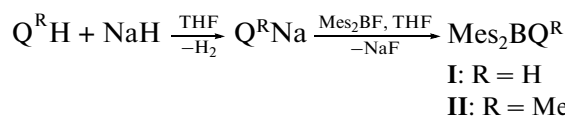
atoms were placed in geometrically calculated positions and refined in the riding model. The crystallographic characteristics and the main refinement parameters are presented in Table 1.

The crystallographic information was deposited with the Cambridge Crystallographic Data Centre (CIF files 1051351 (**I**) and 1051352 (**II**); deposit@ccdc.cam.ac.uk or <http://www.ccdc.cam.ac.uk>).

Preparation of OLED devices. A glass plate with the supported ITO layer (120 nm, 15 Ohm/cm²) (Lum Tec) playing the role of an anode was used as a carrier basis for OLED devices with the configuration ITO/PVK: boron complex (12 wt %) (50 nm)/BATH (30 nm)/Alq₃ (30 nm)/Yb (150 nm). The emission layer consisting of a mixture of PVK and a boron complex was deposited from a solution of the components in CH_2Cl_2 (5 mg/mL) on a Spincoat G3-8 centrifuge (3000 rpm, 30 s) and dried in vacuo at 70°C for 3 h. The layer thickness was determined using a META-900 ellipsometer. The hole-blocking layer BATH, electron-transporting layer Alq₃, and Yb layer acting as a cathode were deposited by evaporation in vacuo (10^{-6} mmHg) from separated thermoresistive evaporators. The layer thickness was monitored with a calibrated quartz resonator. The active surface area of the devices was a circle with a diameter of 5 mm.

RESULTS AND DISCUSSION

Boron complexes **I** and **II** were synthesized by the reaction of sodium salt of the corresponding 8-hydroxyquinoline with fluorodimesitylborane according to the scheme



Compounds **I** and **II** were obtained in high yields of 88–96% as light yellow crystalline air-stable substances highly soluble in CH_2Cl_2 , THF, and toluene and poorly soluble in hexane. The data of IR and NMR spectroscopy correspond to the formulas presented in the scheme.

The structures of the synthesized boron complexes were determined by X-ray diffraction analysis. The coordination sphere of the B(1) atom in compound **I** is a distorted tetrahedron (Fig. 1a, Table 2).

The angles between the substituents at the boron atom vary in a range of 97.1(2)°–117.9(2)°. The B(1)–C(Mes) (1.620(3) and 1.632(4) Å) distances are close to the sum of covalent radii of boron and carbon (1.61 Å [16]). The B(1)–O(1) bond length (1.545(3) Å) is also close to the sum of covalent radii of B and O (1.56 Å [16]). The B(1)–N(1) distance (1.642(3) Å) is somewhat longer than the sum of covalent radii of B and N (1.57 Å [16]) but is substantially

Table 1. Selected crystallographic data and the X-ray diffraction experimental and refinement parameters for compounds **I** and **II**

| Parameter | Value | |
|---|---|---|
| | I | II |
| <i>FW</i> | 393.31 | 407.34 |
| Temperature, K | 100(2) | 150(2) |
| Crystal size, mm | 0.15 × 0.13 × 0.10 | 0.40 × 0.40 × 0.10 |
| Crystal system | Orthorhombic | Monoclinic |
| Space group | <i>Pna2</i> ₁ | <i>P2</i> ₁ / <i>ñ</i> |
| <i>a</i> , Å | 14.8997(18) | 13.4302(3) |
| <i>b</i> , Å | 10.4573(13) | 10.77095(16) |
| <i>c</i> , Å | 13.6684(17) | 16.9746(3) |
| β, deg | 90 | 108.355(2) |
| <i>V</i> , Å ³ | 2129.7(5) | 2330.55(8) |
| <i>Z</i> | 4 | 4 |
| ρ _{calcd} , g/cm ⁻³ | 1.227 | 1.161 |
| μ, mm ⁻¹ | 0.073 | 0.069 |
| <i>F</i> (000) | 840 | 872 |
| Scan θ range, deg | 2.379–26.999 | 3.00–30.00 |
| Index ranges | −19 ≤ <i>h</i> ≤ 19, −13 ≤ <i>k</i> ≤ 13, −17 ≤ <i>l</i> ≤ 17 | −18 ≤ <i>h</i> ≤ 18, −15 ≤ <i>k</i> ≤ 15, −23 ≤ <i>l</i> ≤ 23 |
| Total number of reflections | 21324 | 47574 |
| Number of independent reflections (<i>R</i> _{int}) | 4630 (0.0576) | 6770 (0.0482) |
| Goodness-of-fit | 1.049 | 1.064 |
| <i>R</i> (<i>I</i> > 2σ(<i>I</i>)) | <i>R</i> ₁ = 0.0479, <i>wR</i> ₂ = 0.1023 | <i>R</i> ₁ = 0.0506, <i>wR</i> ₂ = 0.1303 |
| <i>R</i> (all data) | <i>R</i> ₁ = 0.0657, <i>wR</i> ₂ = 0.1077 | <i>R</i> ₁ = 0.0696, <i>wR</i> ₂ = 0.1389 |
| Δρ _{max} /Δρ _{min} , e Å ⁻³ | 0.338/−0.178 | 0.403/−0.193 |

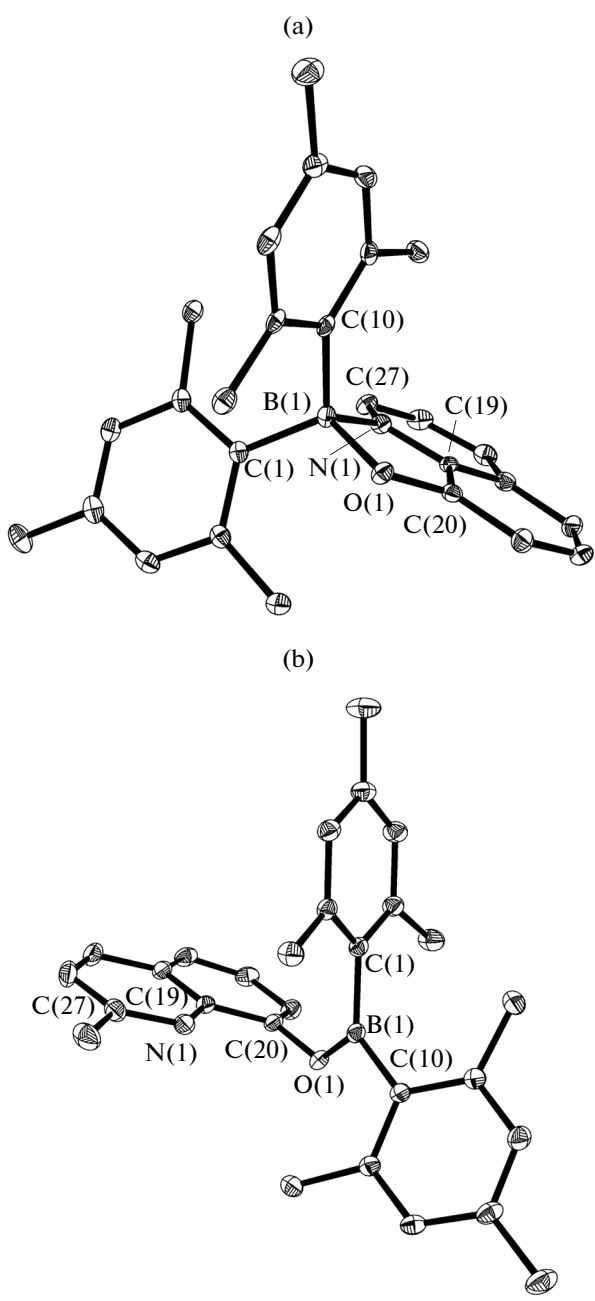


Fig. 1. Molecular structures of complexes (a) **I** and (b) **II** with 30% probability ellipsoids. Hydrogen atoms are omitted.

shorter than the sum of the van der Waals radii of their atoms (3.35 Å [16]).

The B(1) atom in compound **II** has a trigonal coordination unusual for the boron oxyquinoline complexes (Fig. 1b, Table 2).

The average shift of the O(1), C(1), C(10), and B(1) atoms from the plane is 0.015 Å. The sum of angles between the substituents at the B(1) atom is 359.8°. The monodentate methoxyquinoline ligand

is coordinated to the boron atom by the O(1) atom. The B(1)–O(1) distance in compound **II** (1.374(2) Å) is noticeably shorter than B(1)–O(1) in compound **I** (1.545(3) Å). The B(1)–C(Mes) distances in compound **II** (1.581(2) and 1.585(2) Å) are shorter than similar distances in complex **I** (1.620(3), 1.632(4) Å).

The study of the photophysical properties of complexes **I** and **II** show that their absorption spectra are similar to the spectra of the known diphenylboron derivatives Ph_2BQ^R [6] and contain bands that can be attributed to the $\pi \rightarrow \pi^*$ transitions in the aromatic systems of the mesityl rings and oxyquinoline fragments (240–290 nm) and to the intraligand charge-transfer (ILCT) transition in the oxyquinoline fragment (355–370 nm) [17] (Fig. 2, Table 3).

The PL spectra of compounds **I** and **II** in both solution and solid state are similar (Fig. 3, Table 3) and contain broad bands with maxima at 510 and 512 nm (**I**) and 499 and 506 nm (**II**) assigned to the ILCT transitions in the oxyquinoline fragment [17]. As in the case of phenyl derivatives Ph_2BQ^R ($R = \text{H}, \text{Me}$) [6], complex **II** containing the methyl group in position 2 of the oxyquinoline fragment exhibits an insignificant blue shift of the emission band. The quantum PL yields of compounds **I** and **II** are close: 56 and 49%, respectively.

Model OLED devices with the configuration ITO(15 Ω/sq)/PVC were manufactured to study the EL properties of complexes **I** and **II**: boron complex (12 wt %) (50 nm)/BATH(30 nm)/Alq₃(30 nm)/Yb(150 nm), where PVK is the hole-transporting material, BATH is the hole-blocking material, and Alq₃ is the electron-transporting material. An attempt to obtain emission layers by the vacuum evaporation method for compounds **I** and **II** was unsuccessful. The films formed were of low quality because, most likely, of the fast crystallization of the compounds on the support. The EL spectra of complexes **I** and **II** and the performance characteristics of the OLED devices based on these complexes are presented in Figs. 4 and 5 and in Table 4.

As can be seen from Fig. 5, the EL spectra of the OLEDs based on complexes **I** and **II** differ substantially. In the case of complex **I**, the spectrum contains broad bands with maxima at 510 and 513 nm, which can be assigned to the ILCT transitions in the oxyquinoline fragment [17]. No luminescence of the carbazole groups is observed even at high applied voltages, indicating the efficient excitation energy transfer from the polymer matrix to the boron complexes following the Förster mechanism [18]. The chromaticity coordinates of the radiation in the CIE (Commision Internationale de l'Eclairage) diagram (Table 4) correspond to the green color and remain unchanged in the whole range of applied voltages.

Table 2. Selected bond lengths and bond angles in complexes **I** and **II**

| Bond | <i>d</i> , Å | |
|---------------|----------------|-----------|
| | I | II |
| B(1)–O(1) | 1.545(3) | 1.374(2) |
| B(1)–N(1) | 1.642(3) | |
| B(1)–C(1) | 1.620(3) | 1.585(2) |
| B(1)–C(10) | 1.632(4) | 1.581(2) |
| O(1)–C(20) | 1.321(3) | 1.384(1) |
| N(1)–C(19) | 1.352(3) | 1.369(2) |
| N(1)–C(27) | 1.322(3) | 1.324(2) |
| Angle | ω , deg | |
| O(1)B(1)C(1) | 117.0(2) | 119.3(1) |
| C(1)B(1)C(10) | 116.3(2) | 126.0(1) |
| C(10)B(1)O(1) | 103.1(2) | 114.5(1) |
| B(1)O(1)C(20) | 111.2(2) | 124.4(1) |
| O(1)B(1)N(1) | 97.1(2) | |
| N(1)B(1)C(1) | 104.4(2) | |
| N(1)B(1)C(10) | 117.9(2) | |

Table 3. Photophysical characteristics of complexes **I** and **II**

| Compound | $\lambda_{\text{max}}^{\text{abs}}$, nm ($\epsilon \times 10^{-3}$, L mol ⁻¹ cm ⁻¹) | $\lambda_{\text{max}}^{\text{em}}$, nm | | Quantum yield in CH_2Cl_2 , % |
|-----------|--|---|--------------------------------------|--|
| | | solid state | in CH_2Cl_2 solution | |
| I | 243 (45.19), 256 sh (23.16), 304 sh (3.62), 360 sh (0.98) | 512 | 510 | 56 |
| II | 244 (49.60), 258 sh (28.21), 304 (9.71), 355 sh (2.60) | 506 | 499 | 49 |

Table 4. Performance characteristics* of the OLEDs based on complexes **I** and **II**

| Compound | Turn on voltage, V** | Maximum brightness, cd/m ² | Maximum current efficiency, cd/A | Maximum power efficiency, Lm/W | Chromaticity coordinates in CIE diagram |
|-----------|----------------------|---------------------------------------|----------------------------------|--------------------------------|---|
| I | 10 | 356 (21 V) | 0.68 (19 V) | 0.12 (19 V) | $x = 0.25$ $y = 0.45$ |
| II | 10 | 36 (28 V) | 0.57 (11 V) | 0.16 (11 V) | $x = 0.40$ $y = 0.37$ |

* The voltage at which the working characteristics were determined is given in parentheses.

** Brightness at 1 cd/m².

The EL spectrum of complex **II** exhibits bands with maxima at 499 and 506 nm caused by the emission of the organoboron compound. Additional bands with maxima at 439, 526, and 620 nm can be due to the emission of excimers of the carbazole groups (439 nm), emission from the triplet state of the carbazole groups (526 nm), and emission of electromers formed by PVK molecules (620 nm) [19]. The superposition of the bands in the EL spectrum of complex **II** results in the fact that the chromaticity coordinates of the radiation (Table 4) are attributed to the white color range.

Thus, new boron complexes **I** and **II** with mesityl and 8-oxyquinoline ligands were synthesized and structurally characterized. The compounds manifested the intense green PL. The model OLED device with the ITO/PVC configuration, boron complex (12 wt %)/BATH/Alq₃/Yb, based on complex **I** generates the green luminescence with a brightness of 356 cd/m², whereas a similar device based on complex **II** generates the white luminescence with a brightness of 36 cd/m².

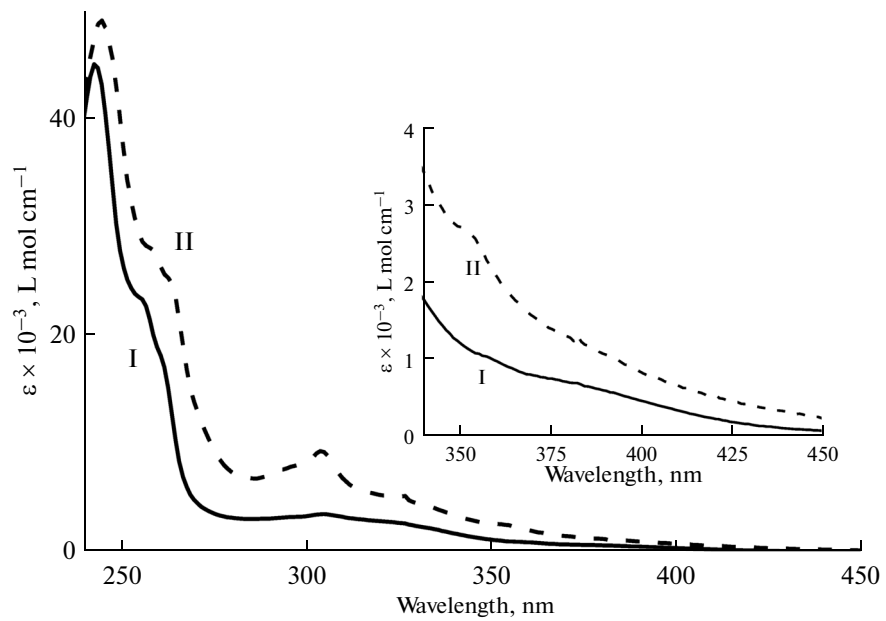


Fig. 2. Absorption spectra of complexes **I** and **II** in CH_2Cl_2 .

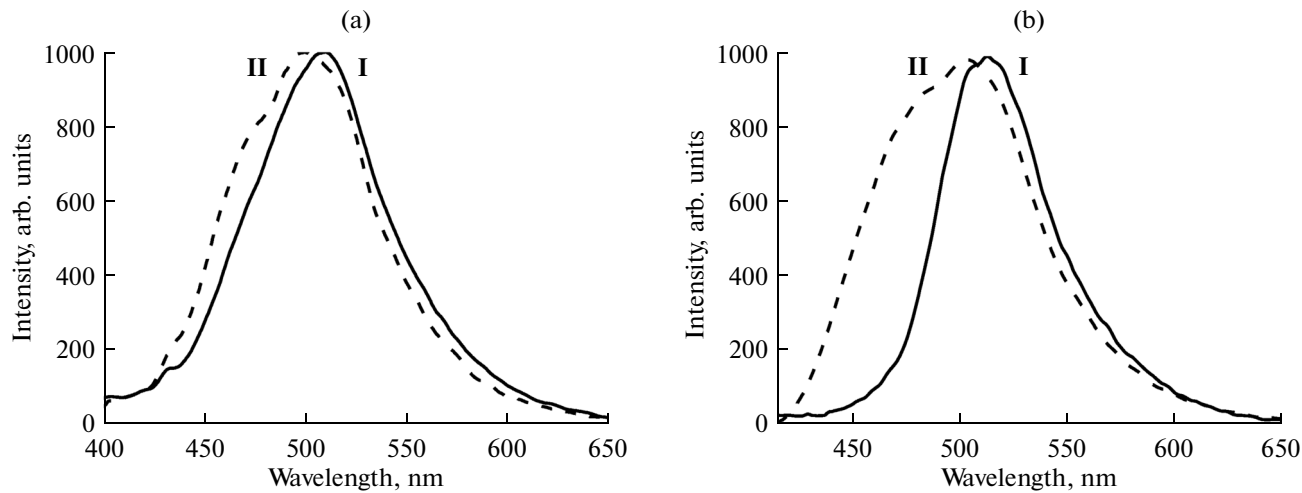


Fig. 3. Normalized PL spectra of complexes **I** and **II** in (a) a CH_2Cl_2 solution ($\sim 1.0 \times 10^{-5}$ mol/L) and (b) the solid state at room temperature ($\lambda_{\text{ex}} = 360$ nm).

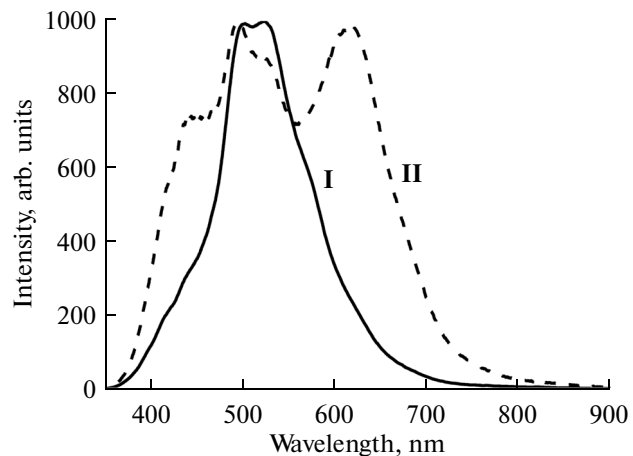


Fig. 4. Normalized EL spectra of the OLEDs based on complexes **I** and **II**.

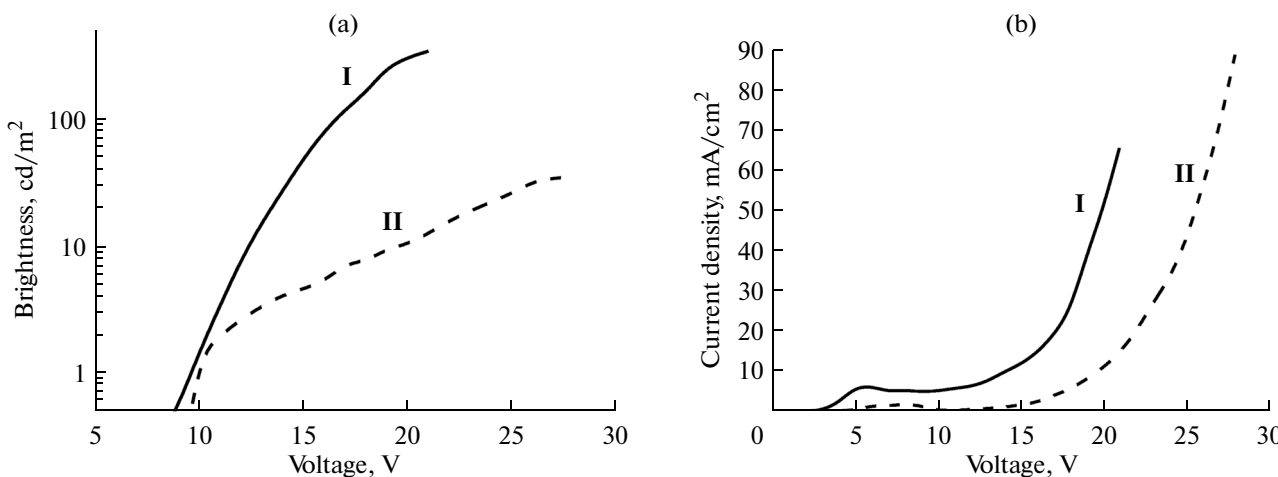


Fig. 5. (a) Luminance-voltage and (b) current density-voltage characteristics of the OLEDs based on complexes I and II.

ACKNOWLEDGMENTS

This work was supported by the Russian Foundation for Basic Research (project no. 15-03-02467-a) and the Ministry of Education and Science of the Russian Federation (project no. 02.V.49.21.0003).

REFERENCES

- Rao, Y.-L. and Wang, S., *Inorg. Chem.*, 2011, vol. 50, p. 12263.
- Li, D., Zhang, H., and Wang, Y., *Chem. Soc. Rev.*, 2013, vol. 42, p. 8416.
- Kalinowski, J., Fattori, V., Cocchi, M., and Williams, J.A.G., *Coord. Chem. Rev.*, 2011, vol. 255.
- Choy, W.C.H., Chan, W.K., and Yuan, Y., *Adv. Mater.*, 2014, vol. 26, p. 5368.
- Hellstrom, S.L., Ugolotti, J., Britovsek, G.J.P., et al., *New J. Chem.*, 2008, vol. 32, p. 1379.
- Anderson, S., Weaver, M.S., and Hudson, A.J., *Synth. Met.*, 2000, vol. 111–112, p. 459.
- Wu, Q., Esteghamatian, M., Hu, N.X., et al., *Chem. Mater.*, 2000, vol. 12, p. 79.
- Ito, A., Kang, Y., Saito, S., et al., *Inorg. Chem.*, 2012, vol. 51, p. 7722.
- Magde, D., Wong, R., and Seybold, P.G., *Photochem. Photobiol.*, 2002, vol. 75, p. 327.
- Demas, J.N. and Crosby, G.A., *J. Phys. Chem.*, 1971, vol. 75, p. 991.
- SAINT. Data Reduction and Correction Program. Version 8.32B*, Madison (WI): Bruker AXS Inc., 2013.
- Data Collection. Reduction and Correction Program. CrysallisPro*, Software Package Agilent Technologies, 2012.
- SADABS-2012/1. Bruker/Siemens Area Detector Absorption Correction Program*, Madison (WI): Bruker AXS Inc., 2012.
- SCALE3 ABSPACK. Empirical Absorption Correction. CrysallisPro*, Software Package Agilent Technologies, 2012.
- Sheldrick, G.M., *SHELXTL. Structure Determination Software Suite. Version 6.12*, Madison (WI): Bruker AXS Inc., 2000, p. 12.
- Batsanov, S.S., *Zh. Neorg. Khim.*, 1991, vol. 36, p. 3015.
- Cheng, Y.-M., Yeh, Y.-S., Ho, M.-L., and Chou, P.-T., *Inorg. Chem.*, 2005, vol. 44, p. 4594.
- Förster, T., *Disc. Faraday Soc.*, 1959, vol. 27, p. 7.
- Ye, T., Chen, J., and Ma, D., *Phys. Chem. Chem. Phys.*, 2010, vol. 12, p. 15410.

Translated by E. Yablonskaya